

# SELF-CONSISTENT METHOD FOR DENSITY ESTIMATION

BY ALBERTO BERNACCHIA\* AND SIMONE PIGOLOTTI†

*Yale University\** and *The Niels Bohr Institute†*

The estimation of a density profile from experimental data points is a challenging problem, usually tackled by plotting a histogram. Prior assumptions on the nature of the density, from its smoothness to the specification of its form, allow the design of accurate estimation procedures, such as Maximum Likelihood. Our aim is to construct a procedure that makes the smallest possible number of assumptions, but still providing an accurate estimate of the density. We introduce the self-consistent estimate: the power spectrum of a candidate density is given, and an estimation procedure is performed on the assumption, to be released *a posteriori*, that the candidate is correct. The self-consistent estimate is defined as a prior candidate density that precisely reproduces itself. Our main result is to derive the exact analytical expression of the self-consistent estimate for any given dataset. Applications of the method do not require any assumption about the form of the density. Moreover, a cutoff frequency emerges naturally from the derivation, so that the estimate does not depend on the subjective choice of parameters, such as a bin size or a kernel bandwidth. We study its application to Gaussian and Cauchy distributions: although the self-consistent estimate is non-parametric, it reaches the theoretical limit of Maximum Likelihood for the scaling of the square error with the dataset size.

**1. Introduction.** Every scientist has encountered the problem of estimating a continuous density from a discrete set of data points. This may happen, for example, when determining a probability distribution from a finite Monte Carlo sample [3], rounding off the shape of a galaxy from a collection of stars [23], or assessing the instantaneous firing rate of a neuron from a discrete set of action potentials [17]. In all those cases, one can adopt two different approaches: either assuming a given functional form for the density *a priori*, specified by a certain number of parameters, or renouncing any prior knowledge (beyond that a density exists and, in some cases, that is smooth). These two approaches lead, respectively, to parametric and non-parametric estimates. We will focus on the latter approach, although we will assume the knowledge of the density as a reasoning tool, to be released *a*

---

*AMS 2000 subject classifications:* Primary 62G07

*Keywords and phrases:* non-parametric statistics, kernel density estimation, binning

*posteriori*.

The most popular non-parametric method is simply plotting a histogram, but more sophisticated procedures have been developed. Kernel Density Estimation (KDE) has been widely studied [27, 21, 28]: instead of counting the number of points in separate bins, KDE constructs a smoothed picture of the data as a superposition of kernel functions centered at the coordinates of data points. More formally, given a sample of  $N$  data points (real numbers), denoted by  $\{X_j\}$  ( $j = 1, \dots, N$ ), the KDE function  $\hat{f}(x)$  is written as

$$(1.1) \quad \hat{f}_{KDE}(x) = \frac{1}{hN} \sum_{j=1}^N K\left(\frac{x - X_j}{h}\right)$$

where  $K(x)$  is the smoothing kernel and  $h$  represents its width (the "bandwidth"). Usually, the choice of  $K(x)$  is not crucial [27], while  $h$ , which controls the degree of smoothing, has to be carefully adjusted: the more concentrated data points are, the less smoothing is necessary in order to obtain a good estimate of their density. An alternative non-parametric method is the "Maximum Penalized Likelihood" (MPL, [13]), also known in the physics literature as a particular regularization of Field Theory [2, 15, 25]: it consists in performing a functional average of densities weighted by their likelihood and by a measure of their smoothness.

In general, each non-parametric method depends on the arbitrary choice of one adjustable parameter, such as the bin size in histograms, the bandwidth in KDE, or the cutoff frequency in MPL and Field Theory. Each of them regularizes the estimate and avoids overfitting of the data points. In most cases this corresponds to low-pass filtering, i.e. cutting the high frequencies inherent to the discrete dataset, and preventing the estimate from merely reproducing a narrow peak at each data point. However, it would be desirable to devise methods involving the least possible number of parameters, since their determination usually involves some specific assumptions on the distribution to be estimated (e.g. varying the cutoff parameter in MPL and Field Theory precisely corresponds to different choices of the bayesian prior [2]). Cross-validation techniques have been previously applied for this purpose [4], but they are computationally expensive and have been seldom applied in the literature.

In this study we show that a self-consistent approach leads to the emergence of a natural cutoff frequency, and an estimate of the density whose performance approaches the theoretical limit of the Maximum Likelihood. We start from the observation, made in ref. [29], that a unique "optimal" convolution kernel can be derived as a function of the power spectrum of the (unknown) density to be estimated. We replicate and extend this result

in Appendix 1, which is of little use, since the power spectrum of the true density is not known *a priori*. However, in Section 2 we exploit it by defining the "self-consistent" estimate as the one whose associated optimal kernel, applied to the sample dataset, returns the estimate itself. Our main result is derive the exact expression of the self-consistent estimate for any given dataset. Beside the insensitive choice of an initial guess, the self-consistent estimate is unique, and no parameters have to be arbitrarily adjusted. In section 3 we test the method on two different problems: the estimates of a Gaussian and a Cauchy distribution, the latter being representative of long-tailed distributions. In both cases we show that the mean integrated square error reaches the optimal theoretical scaling  $\sim N^{-1}$ , i.e. it approaches the performance of parametric estimates, such as Maximum Likelihood, despite the fact that the self-consistent estimate is non-parametric.

**2. The self-consistent estimate.** In this section, we define the self-consistent estimate, we derive its exact expression, and we study its properties. We start from a result derived in ref.[29], that we replicate and extend in Appendix 1. The basic result is that a unique, optimal convolution kernel can be derived as a function of the power spectrum of the density to be estimated, where "optimal" is intended as minimizing the mean integrated square difference between the true density and its estimate.

Given a sample of  $N$  data points (real numbers), denoted by  $\{X_j\}$  ( $j = 1 \dots N$ ), each independently drawn from a probability density distribution  $f(x)$ , we write the estimate as

$$(2.1) \quad \hat{f}(x) = \frac{1}{N} \sum_{j=1}^N K(x - X_j)$$

where we assume  $f, \hat{f} \in L^2$ . Note that this estimate does not depend on any bandwidth  $h$ , contrary to the KDE estimate (1.1). Instead of choosing an arbitrary shape for the kernel  $K$ , and looking for an optimal bandwidth (see e.g. [27]), we rather look for an optimal shape of the kernel. It turns out that the Fourier transform  $\kappa_{opt}(t)$  of the optimal kernel  $K_{opt}(x)$  is equal to (see Appendix 1 and ref.[29])

$$(2.2) \quad \kappa_{opt}(t) = \frac{N}{N - 1 + |\phi(t)|^{-2}}$$

where  $\phi(t)$  is the Fourier transform of the true density  $f(x)$  (characteristic function). The optimal kernel  $K_{opt}(x)$  is symmetric with respect to  $x = 0$ ,

where it takes its maximum value. Note that  $|\phi(t)|$  in Eq.(2.2) requires knowledge of the true density, which is not available, hence Eq.(2.2) cannot be used to compute the estimate in Eq.(2.1) from the sample observations  $\{X_j\}$  alone. We show in the following how we can circumvent this problem by a self-consistent approach. Eq.(2.2) has been previously derived in ref.[29], and has represented a benchmark for assessing the performance of specific kernels [8], as well as for constructing blockwise estimators [10].

Although Eq.(2.2) cannot be used to compute the density estimate, we make a step further and we write the Fourier transform  $\hat{\phi}(t)$  of the density estimate  $\hat{f}(x)$  in Eq.(2.1), using the transformed kernel (2.2), as

$$(2.3) \quad \hat{\phi}(t) = \Delta(t) \frac{N}{N-1 + |\phi(t)|^{-2}}.$$

where  $\Delta(t)$  is the transform of a sum of Dirac delta functions centered at data points, i.e.

$$(2.4) \quad \Delta(t) = \frac{1}{N} \sum_{j=1}^N e^{itX_j}$$

In what follows, we construct a bootstrap procedure based on Eq.(2.3). Our goal is to determine the fixed point of this procedure analytically, so that practical applications of the method will not involve the computational expense required by bootstrapping. We replace the unknown term  $\phi$  in Eq.(2.3) with an initial guess  $\hat{\phi}_0$ , and we denote the resulting estimate as  $\hat{\phi}_1$ . Then, we try to obtain an improved estimate  $\hat{\phi}_2$  by using a kernel which is optimal for  $\hat{\phi}_1$ . By iterating this procedure, we construct the following sequence of estimates

$$(2.5) \quad \hat{\phi}_{n+1} = \frac{N\Delta}{N-1 + |\hat{\phi}_n|^{-2}}.$$

We search for a fixed point of the iteration, namely an estimate  $\hat{\phi}_{sc}$  for which

$$(2.6) \quad \hat{\phi}_{sc} = \frac{N\Delta}{N-1 + |\hat{\phi}_{sc}|^{-2}}$$

This coincides with the density whose corresponding optimal kernel applied to the data sample gives back the density itself. We call a solution of Eq.(2.6)

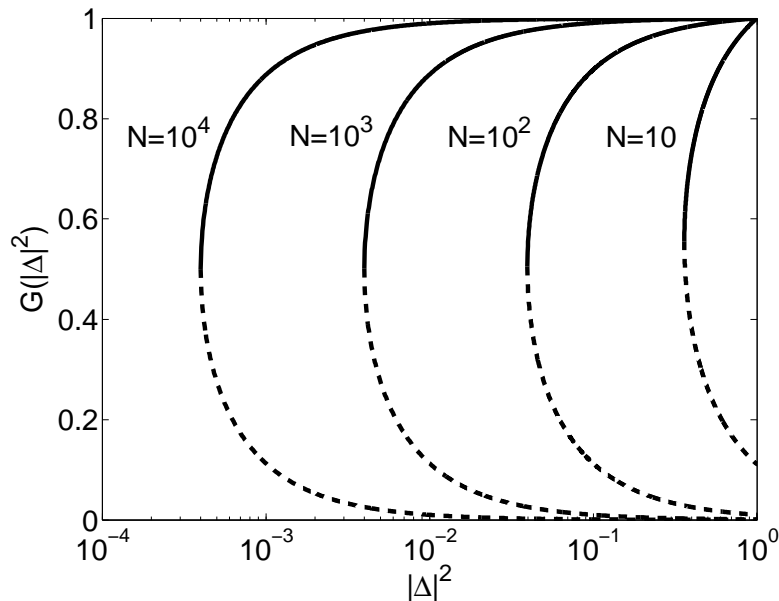


FIG 1. Amplitude gain function of the self-consistent estimate, for different values of the sample size  $N$ . The stable  $G^+$  is shown in full line, while the unstable  $G^-$  is shown in dashed line. The amplitude gain is always smaller than 1, except for  $|\Delta|^2 = 1$ .  $G^+$  tends to one and  $G^-$  tends to zero for large values of  $N$ .

”self-consistent estimate”. In Appendix 2 we show that the above iteration has three solutions and we study their stability. One solution is the trivial null solution, i.e.  $\hat{\phi}_{sc} = 0$ , while the other two, denoted by the superscript  $\pm$ , are equal to

$$(2.7) \quad \hat{\phi}^{\pm}(t) = \Delta(t) G^{\pm}(|\Delta(t)|^2)$$

where  $G$  is the amplitude gain function of the estimate, expressing its filtering properties (as much as the kernel  $\kappa$  above), and is written as

$$(2.8) \quad G^{\pm}(|\Delta|^2) = \frac{2}{N|\Delta|^2 \mp |\Delta| \sqrt{N^2|\Delta|^2 - 4N + 4}}$$

The amplitude gain  $G$  is plotted in Fig. 1. It describes the relative amount of power of the data source that is maintained by the self-consistent estimate. Eqs. (2.7,2.8) constitute our main result.

As shown in Fig. 1, the solutions corresponding to  $G^\pm$  exist for frequencies  $t$  whose amplitude  $|\Delta(t)|$ , computed from the data, is greater than a threshold depending on  $N$ , that is

$$(2.9) \quad |\Delta|^2 \geq \frac{4(N-1)}{N^2}$$

This condition sets a threshold below which the only solution is  $\hat{\phi}_{sc} = 0$ . Hence, the contribution of small amplitude waves is neglected, and this automatically determines the range of frequencies to be considered for the estimate. In most practical situations, the filter will cut the high frequency bands, but the filter is not constrained to be low-pass, and it can rather select different frequency bands.

Of the three solutions  $0$ ,  $\hat{\phi}^+$  and  $\hat{\phi}^-$ , the first two are stable while the latter is unstable (see Appendix 2). When  $|\Delta|^2 < \frac{4(N-1)}{N^2}$ , the only solution is  $\hat{\phi}_{sc} = 0$  and is globally stable, while for  $|\Delta|^2 \geq \frac{4(N-1)}{N^2}$  there are two stable solutions,  $\hat{\phi}_{sc} = \hat{\phi}^+$  and  $\hat{\phi}_{sc} = 0$ . In the latter case, the initial guess  $\hat{\phi}_0$  will evolve, following Eq.(2.5), towards one of the two solutions, depending on whether its absolute value is larger or smaller than the saddle point value  $|\hat{\phi}^-|$ . Because the saddle point is close to zero ( $|\hat{\phi}^-| \simeq \frac{1}{N|\Delta|}$  for large  $N$ ), a natural choice, eliminating the dependence on the initial guess, would be to select  $\hat{\phi}_{sc} = \hat{\phi}^+$  for all frequencies whose amplitudes are above the threshold, and  $\hat{\phi}_{sc} = 0$  otherwise. However, we show in Appendix 3 that this choice would correspond to non-summable both initial guess and estimate  $\hat{\phi}_0, \hat{\phi}_{sc} \notin L^2$ , implying the the anti-trasform of the estimate does not exist. Further, we show that a summable initial guess  $\hat{\phi}_0 \in L^2$  implies a summable self-consistent estimate  $\hat{\phi}_{sc} \in L^2$ , such that it can be antitransformed back to the real estimate.

Since most amplitudes will fall below threshold for large  $|t|$ , we assume that reasonable choices of an initial guess  $\hat{\phi}_0 \in L^2$  will converge to similar fixed points  $\hat{\phi}_{sc}$  (in the sense of  $L^2$  measure). A simple choice is to consider  $\hat{\phi}_{sc}(t) = 0$  for large  $|t|$  and  $\hat{\phi}_{sc}(t) = \hat{\phi}^+(t)$  (above threshold, zero otherwise) for small  $|t|$ . We discuss in the next section how to determine a cutoff by means of the threshold given in (2.9). Adopting such choice, the function  $\hat{\phi}_{sc}$  can be antitransformed back to the self-consistent estimate in the real space, i.e.

$$(2.10) \quad \hat{f}_{sc}(x) = \frac{1}{2\pi} \int_{-\infty}^{\infty} dt e^{-itx} \hat{\phi}_{sc}(t)$$

Applications of the method are considered in the next section. The self-consistent estimate is normalized by construction, i.e.  $\int_{-\infty}^{+\infty} dx \hat{f}_{sc}(x) = 1$  or, equivalently,  $\hat{\phi}_{sc}(0) = 1$  (note that  $\Delta(0) = 1$  and  $G^+(1) = 1$ ), and is defined only for  $N > 2$ , because  $|\Delta| \leq 1$ . Beside the zero frequency that is kept intact (corresponding to the normalization condition),  $G^+$  tends to attenuate all other frequencies ( $G \leq 1$ ). Because  $\hat{\phi}_{sc}(t)$  is continuous and infinitely differentiable at  $t = 0$ , all the moments of the self-consistent estimate  $\hat{f}_{sc}(x)$  exist. However,  $\hat{\phi}_{sc}(t)$  is discontinuous for some  $t \neq 0$ , and this may determine slowly decaying oscillations in the tails of  $\hat{f}_{sc}(x)$  (see below). The mean and variance of  $\hat{f}_{sc}(x)$  are equal to (see Appendix 2)

$$(2.11) \quad E(x) = \frac{1}{N} \sum_{j=1}^N X_j$$

$$(2.12) \quad \text{Var}(x) = \frac{1}{N-2} \sum_{j=1}^N (X_j - E(x))^2$$

While the mean is equal to the sample mean, the variance is larger than the sample variance as well as than its unbiased estimator, which is normalized by  $\frac{1}{N-1}$  instead of  $\frac{1}{N-2}$ .

A drawback of the self-consistent estimate is that it is not guaranteed to be non-negative, while a true density is, by construction, a non-negative entity (note that  $|\hat{\phi}_{sc}(t)|^2 \leq 1$  holds from Eq.(2.7), because  $|\Delta|^2 \leq 1$  and  $|G|^2 \leq 1$ , but that is a necessary and not sufficient condition for  $\hat{f}_{sc}(x)$  to be non-negative). In general, the restriction to a strictly non-negative estimate has a cost, in terms of the mean integrated square error, quantified by the decay exponent  $\alpha$  of the error as a function of the sample size,  $E(I) \propto N^{-\alpha}$ . Among the estimation procedures that properly give non-negative results, histograms, MPL and Field Theories have  $\alpha = 2/3$  [2, 15], while positive kernels in KDE do better with an  $\alpha = 4/5$  [27]. Applications of estimates that are allowed to be negative reach better performance, like "m-th order" kernels [28, 14, 1], that have  $\alpha = \frac{2m}{2m+1}$ , while the optimal estimate (4.9) and infinite order kernels [9], such as the "sinc" kernel [8, 25], yield  $\alpha = 1$ , besides logarithmic terms. Hence, releasing the requirement of a non-negative density estimate allows one to gain a better performance. The optimal scaling  $\alpha = 1$  is also reached by parametric estimators, such as Maximum Likelihood which are, however, strictly non-negative. We present below numerical results suggesting that the self-consistent estimate (2.7) also reaches  $\alpha = 1$ . While it is not guaranteed to be non-negative, we seldom

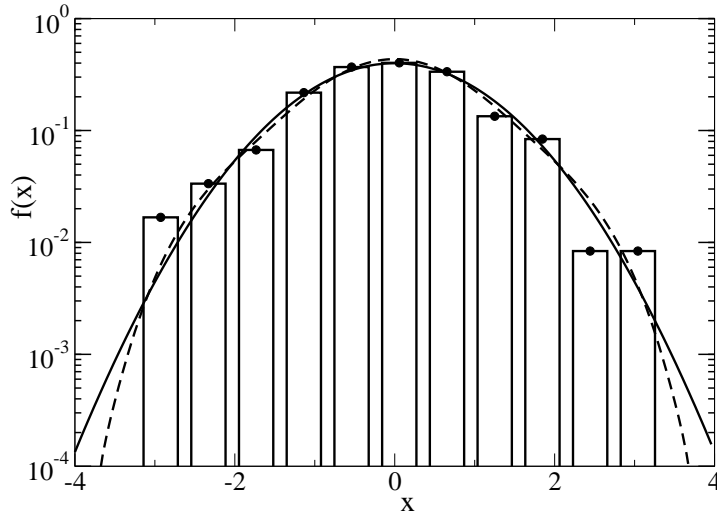


FIG 2. Illustrative example of an estimate of a Gaussian density from  $N = 200$  sample points. The true density is given by the full line. The dashed line is the self-consistent estimate, compared with a histogram having optimal binwidth [26].

observed negative values in simulations. Those can be corrected without any error cost [11], by translating the estimate downward until the positive part is normalized to one, and setting to zero the negative part.

**3. Applications to artificial data.** In this section we apply the self-consistent estimate  $\hat{f}_{sc}(x)$ , constructed from a sample of  $N$  data points  $\{X_j\}$  ( $j = 1 \dots N$ ) by using Eq.(2.10). We apply the self-consistent estimate to artificial datasets generated from Gaussian and Cauchy distributions.

As we discussed in the previous section, the self-consistent estimate depends on the choice of a summable initial guess. However, this dependence is weak, since the amplitude of frequencies computed from data is below the threshold for most of the high frequencies, and they would be neglected. In the following, we choose the non-zero solution  $\hat{\phi}^+$ , where above threshold, only for frequencies in a symmetric interval  $[-t_{max}, t_{max}]$ , such that the measure of the set of points for which the inequality (2.9) holds is one half of the interval. Additional simulations show that changing this criterion has small effects (doubling the interval has a less than 10% effect on the error).

The first example we present is the estimate of a Gaussian distribution,  $f(x) = e^{-x^2/2}/\sqrt{2\pi}$ . For illustrative purposes, we present in Fig. 2 the application of the self-consistent estimate to a single sample of  $N = 200$  points: with respect to a histogram (where we chose the optimal binwidth, see [26]),



it appears to be particularly accurate for assessing the density of the tails of the distribution. We explore more systematically the performance of the self-consistent estimate by generating 100 samples, each composed of  $N$  points randomly and independently drawn from  $f(x)$ . The performance is evaluated in terms of the mean integrated square error, Eq.(4.2), where the mean is calculated over the 100 sample realizations. We compare the performances of different estimation methods for different values of  $N$ , by repeating the above procedure for each value of  $N$ , ranging from  $10^2$  to  $10^6$ , and for each one of the methods listed below.

Fig. 3 shows the error  $E(I)$  as a function of the sample size  $N$ , for the self-consistent estimate (SC), the optimal kernel estimate (OPT), the kernel density estimate (KDE), and the Maximum Likelihood estimate (ML). Lines show exact formulas, while points are results of the simulations described above. We used a Gaussian kernel for KDE, and the exact expression for the error is

$$\begin{aligned} E(I_{KDE}) &= \frac{1}{2\sqrt{\pi}} \left( \frac{1}{Nh} - \frac{1}{N\sqrt{1+h^2}} + 1 - \frac{2}{\sqrt{1+h^2/2}} + \frac{1}{\sqrt{1+h^2}} \right) \simeq \\ &\simeq \frac{1}{2\sqrt{\pi}} \left( \frac{1}{Nh} + \frac{3h^4}{16} \right) \end{aligned}$$

We set the asymptotic optimal bandwidth  $h \simeq 1.06 * \sigma * N^{-1/5}$  (see Eq.(3.28) in [27]), with  $\sigma = 1$ , and the error is  $E(I_{KDE}) \simeq 0.33 * N^{-4/5}$ . The error of the optimal estimate is given by Eq.(4.10), and for a Gaussian density is equal to

$$(3.1) \quad E(I_{OPT}) = \frac{\frac{N}{2\sqrt{\pi(N-1)}} \text{Li}_{\frac{1}{2}}(1-N) - 1}{N-1} \simeq \frac{\sqrt{\log(N)}}{\pi N}$$

where  $\text{Li}$  is the Polylogarithm function, defined by  $\text{Li}_s(z) = \sum_{k=1}^{\infty} \frac{z^k}{k^s}$ . This scales as  $N^{-1}$ , up to logarithmic corrections. The error for ML is equal to

$$(3.2) \quad E(I_{ML}) = \frac{7}{16\sqrt{\pi}} N^{-1}$$

The error of the self-consistent estimate is generally smaller than the KDE estimate, and it approaches the theoretical line of the OPT estimate, which scales as ML (apart for logarithmic corrections). We stress that both Maximum Likelihood and the optimal estimate require prior knowledge of

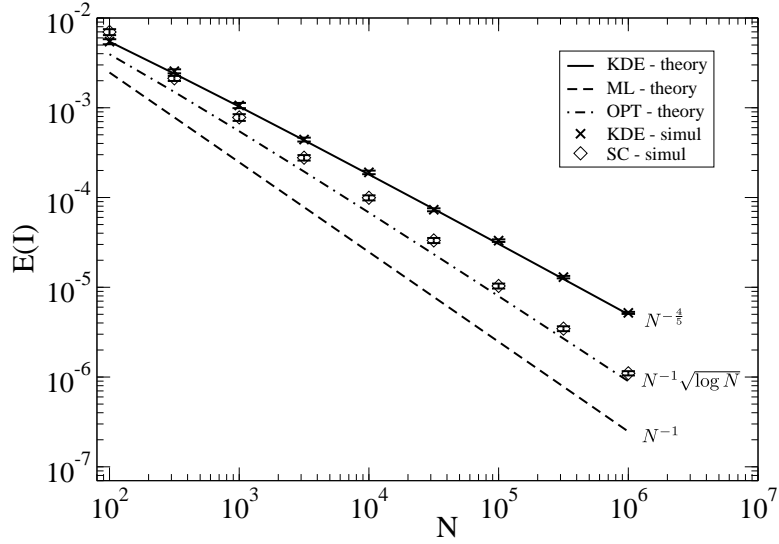


FIG 3. Mean integrated square error  $E(I)$  for the estimate of a Gaussian distribution, as a function of the sample size  $N$ . Lines are theoretical predictions and points are simulations, each point is an average over 100 realizations of the datasets; bars are standard errors. Legend: (KDE) kernel density estimate (ML) maximum likelihood, (OPT) optimal kernel estimate, (SC) self-consistent estimate. Notice that only SC is applied without any prior knowledge: ML assumes that the density is Gaussian, OPT requires its power spectrum in advance, and the bandwidth in KDE is optimized for a Gaussian distribution, i.e.  $h = 1.06 * \sigma * N^{-1/5}$  with  $\sigma = 1$  (see Eq.(3.28) in [27])

the density to be estimated. The former needs to know that the density is Gaussian, the latter needs its spectrum in advance, while the self-consistent method achieves the same scaling without any prior assumption.

The second application is the estimate of a Cauchy distribution,  $f(x) = [\pi(1+x^2)]^{-1}$ . The interest of this case comes from the difficulties of binning long-tailed distributions, especially when the variance diverges. By using a Gaussian kernel, the error for KDE is given by

$$\begin{aligned} E(I_{KDE}) &= \frac{1}{2\sqrt{\pi}Nh} + \frac{1}{2\pi} + \frac{N-1}{2\sqrt{\pi}Nh} e^{h^{-2}} \operatorname{erfc}(h^{-1}) - \frac{\sqrt{2}}{\sqrt{\pi}h} e^{2h^{-2}} \operatorname{erfc}(\sqrt{2}h^{-1}) \simeq \\ &\simeq \frac{1}{2\sqrt{\pi}Nh} + \frac{3h^4}{16\pi} \end{aligned}$$

We set the bandwidth  $h = 0.79 * iq * N^{-1/5}$  (see Eq.(3.29) in [27]), with  $iq = 2$ , that gives  $E(I_{KDE}) \simeq 0.55 * N^{-4/5}$ . The error of the optimal estimate, Eq.(4.10), in the case of the Cauchy distribution, yields

$$(3.3) \quad E(I_{OPT}) = \frac{\frac{N}{2\pi(N-1)} \log(N) - \frac{1}{2\pi}}{N-1} \simeq \frac{\log(N)}{2\pi N}$$

which, again, scales as  $N^{-1}$ .

In order to cope with long-tailed distributions, KDE methods have been generalized to the "adaptive" kernel, which allows the bandwidth to vary locally according to a first estimate of the density [27, 16]. In Fig. 4 we show the mean square error as a function of  $N$  for the standard KDE, the adaptive kernel estimate (ADAPT), the SC and OPT estimates. For small datasets, the adaptive kernel method performs best. However, the self-consistent method still shows better scaling with  $N$ , and its error is lower for large sample sizes, with a crossover occurring for  $N$  between  $10^4$  and  $10^5$ . Again, the error of the self-consistent estimate approaches the optimal theoretical error, and seems to have the same scaling  $\sim N^{-1}$ . We stress that the adaptive method requires some prior knowledge: it is used when one knows that the distribution is long-tailed and, again, the optimal estimate requires prior knowledge of its power spectrum. Conversely, we applied the self-consistent method blindly, in the same way as we did in the Gaussian case.

Finally, a generic non-adaptive estimate can be converted into an adaptive one by a transformation of  $x$  leading to a space with uniform measure [24, 22], and the application of this procedure to the self-consistent estimate will be the subject of a future study.

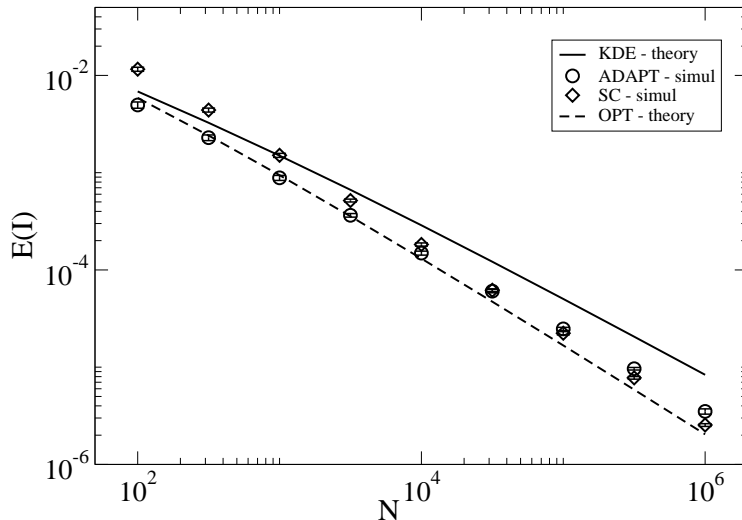


FIG 4. Mean square error  $E(I)$  for the estimate of a Cauchy distribution as a function of the sample size  $N$ . Lines are theoretical predictions and points are simulations, each point is an average over 100 realizations of the dataset; bars are standard errors. Legend: (KDE) kernel density estimate, (ADAPT) adaptive kernel estimate, (SC) self-consistent estimate, (opt) optimal kernel estimate. Notice that only SC is applied without any prior knowledge: ADAPT applies to long-tailed distributions, OPT requires the power spectrum of the true density in advance, and the bandwidth in KDE and ADAPT requires prior knowledge of the interquartile distance of the distribution, i.e.  $h = 0.79 * iq * N^{-1/5}$  with  $iq = 2$  (see Eq.(3.29) in [27])

**4. Discussion.** We presented a method that estimates a density in a self-consistent way from a finite, empirical sample. Beside the insensitive choice of an initial guess, this approach produces a unique estimate where no parameters have to be adjusted, and the only prior is the belief in the self-consistent procedure, that allows avoiding overfitting. On the other hand, the cases in which there exists a widely accepted theoretical framework for the system at hand would rather point to a bayesian, parametric approach in which a specific form for the density is postulated.

The self-consistent estimate approaches the theoretical bound for the error, it has a better scaling than existing methods and is therefore preferable, especially for large datasets. A filter emerges naturally in the derivation, as a function of the data sample, and avoids overfitting of the data. When long tails or power-law behavior is suspected, one is tempted to use logarithmic binning, but that has been shown to be highly inaccurate [7, 12], and sometimes to lead to the conclusion that the density has power-law tails even when it does not. The self-consistent method constitutes a good alternative

when there are no solid theoretical grounds to assume (or discard) a power law.

The method is computationally cheap, and could be applied concretely to any problem in which a density is sampled and there is no prior knowledge of its functional shape. For instance, the mode of the instantaneous firing rate of a cortical neuron may indicate whether the choice of a behaving monkey is triggered by a memorized object or a spatial cue [20]. Another application could be the density estimate of the spacings between zeros of the Riemann Zeta function, based on very large numerical dataset, which could help investigate the related mathematical conjectures [19]. Finally, the method can be used to analyze samples obtained from Monte Carlo simulations [3].

We remark that the method could not be applied to the case of discrete distributions, in which data points are integer numbers. In general, when data points are uniformly spaced by multiples of any constant length, the Fourier transform of their density is periodic. An amplitude threshold and a cutoff frequency would be meaningless in that case, and this would preclude any practical application. However, when data points are integers, there is usually no need for filtering, and it is sufficient to use a histogram, counting the occurrences of each integer.

Finally, a straightforward generalization is to consider a finite interval  $[a, b]$  instead of the entire line  $(-\infty, +\infty)$ , by using Fourier series instead of Fourier transforms. Another possibility is to apply the method to high-dimensional distributions. In our derivation, the relevant variables are scalar quantities, and the  $d$ -dimensional analogy is obtained by using the  $d$ -dimensional Fourier transform, i.e. by performing the integral  $\frac{1}{(2\pi)^d} \int_{\mathbb{R}^d} dt^d$  instead of  $\frac{1}{2\pi} \int_{\mathbb{R}} dt$ . Among many possible implementations, the method could be then applied to the analysis of multielectrode neuronal recordings [6], multivariate financial data [5], and reconstruction of Ramachandran angle distributions [18].

**Appendix 1: The optimal kernel.** In this section, we show that a unique "optimal" convolution kernel can be derived as a function of the power spectrum of the density to be estimated. A similar result has been presented in [29]. Given a sample of  $N$  data points (real numbers), denoted by  $\{X_j\}$  ( $j = 1 \dots N$ ), each independently drawn from a probability density distribution  $f(x)$ , we write the estimate as

$$(4.1) \quad \hat{f}(x) = \frac{1}{N} \sum_{j=1}^N K(x - X_j)$$

The true density  $f$  is assumed to be normalized, i.e.  $\int_{-\infty}^{+\infty} dx f(x) = 1$ .

We look for a kernel  $K(x)$  such that the estimate (4.1) minimizes the mean integrated square error

$$(4.2) \quad E(I) = E \int_{-\infty}^{+\infty} dx [\hat{f}(x) - f(x)]^2$$

where  $E(\cdot)$  denotes an average over all the possible realizations of the data sample  $\{X_j\}$ . In order to minimize (4.2), we follow a procedure for signal deconvolution (the Wiener filter [30]). We introduce the Fourier transform of the unknown density (the characteristic function)

$$(4.3) \quad \phi(t) = \int_{-\infty}^{+\infty} dx e^{itx} f(x)$$

The normalization condition now reads  $\phi(0) = 1$ . We also call  $\hat{\phi}(t)$  and  $\kappa(t)$  the Fourier transforms of the estimate  $\hat{f}(x)$  and of the kernel  $K(x)$  respectively. The mean integrated square error (4.2) corresponds to the mean square distance between the true density  $f$  and the estimate  $\hat{f}$ , in terms of the Euclidean metric in the Hilbert space  $L^2$  (we assume  $f, \hat{f}, \phi, \hat{\phi} \in L^2$ ). By means of Parseval's theorem, we rewrite (4.2) in Fourier space as

$$(4.4) \quad E(I) = \frac{1}{2\pi} E \int_{-\infty}^{+\infty} dt |\hat{\phi}(t) - \phi(t)|^2$$

It is straightforward to perform the average in Fourier space. Applying the convolution theorem to Eq.(4.1), the transformed estimate is equal to  $\hat{\phi}(t) = \kappa(t)\Delta(t)$ , where

$$(4.5) \quad \Delta(t) = \frac{1}{N} \sum_{j=1}^N e^{itX_j}$$

is the transform of a sum of Dirac delta functions centered at data points (note that  $\Delta \notin L^2$  for any finite value of  $N$ , but  $\hat{\phi} \in L^2$  by assumption). Using  $E(\Delta) = \phi$ , and  $E(|\Delta|^2) = |\phi|^2 + N^{-1}(1 - |\phi|^2)$ , we can rewrite the error as

$$(4.6) \quad E(I) = \frac{1}{2\pi} \int_{-\infty}^{+\infty} dt \{N^{-1}|\kappa|^2 (1 - |\phi|^2) + |\phi|^2 |1 - \kappa|^2\}.$$

Since  $f(x)$  is a density, it is normalized and non-negative, which implies  $|\phi|^2 \leq 1$ . Then, the first term in the integral, proportional to  $1/N$ , is non-negative: it corresponds to the error due to the finite size of the sample, while the second term does not depend on  $N$ . These two sources of error are known as error variance and error bias respectively [27]. Among the possible choices of the kernel, we search for the one minimizing the mean integrated square error. Since Eq.(4.6) is quadratic in  $\kappa$ , it is straightforward to find its global minimum, by setting to zero the functional derivative of  $E(I)$  with respect to  $\kappa$ , i.e.

$$(4.7) \quad 2\pi \frac{\delta E(I)}{\delta \kappa^*} = N^{-1} \kappa (1 - |\phi|^2) - |\phi|^2 (1 - \kappa) = 0$$

where the asterisk denotes complex conjugate. This yields a unique, optimal kernel, which in Fourier space reads

$$(4.8) \quad \kappa_{opt}(t) = \frac{N}{N - 1 + |\phi(t)|^{-2}}$$

The optimal kernel satisfies the normalization condition  $\kappa_{opt}(0) = 1$ , because  $\phi(0) = 1$ , and is a real function. Since the density  $f$  is real, then  $|\phi(t)| = |\phi(-t)|$ , which implies that  $\kappa_{opt}(t)$  is an even function. Then its antitransform  $K_{opt}(x)$ , the optimal kernel in the real space, is also real and even and, because expression (4.8) is non-negative,  $K_{opt}(x)$  takes the maximum value at  $x = 0$ , i.e. at the coordinate of each data point in Eq.(4.1).

Using the expression for the transformed optimal kernel, Eq.(4.8), we rewrite the estimate, Eq.(4.1), in Fourier space, as

$$(4.9) \quad \hat{\phi}(t) = \Delta(t) \frac{N}{N - 1 + |\phi(t)|^{-2}}.$$

which we call the "optimal estimate". The optimal estimate satisfies the normalization condition,  $\hat{\phi}(0) = 1$ , because  $\Delta(0) = 1$  and  $\phi(0) = 1$ . For infinite sample size ( $N \rightarrow \infty$ ), the optimal estimate reduces to the true density with probability one, i.e.  $\hat{\phi}(t) \rightarrow \phi(t)$ , because the law of large numbers implies  $\Delta(t) \rightarrow \phi(t)$  (strong convergence), while the fractional term, the kernel, tends to one. This is because an infinite sample would reproduce the true density itself, without the need of any transformation of the data. For finite  $N$ , the optimal estimate cuts the frequencies that have less power in the true density, and hence are more subject to noise, i.e. frequencies  $t$  whose power is of the order  $|\phi(t)|^2 \simeq 1/N$  or less.

The above procedure is analogous to the derivation of the Wiener filter for signal deconvolution [30]: the prior knowledge of the power spectrum of both the signal, the unknown density, and the noise establishes a unique criterion for optimal signal to noise separation (note that, once the signal spectrum is given,  $|E(\Delta)|^2 = |\phi|^2$ , the assumption of independency of data points allows the noise spectrum to be written as a function of the signal, i.e.  $E(|\Delta|^2) - |E(\Delta)|^2 = N^{-1}(1 - |\phi|^2)$ ).

We conclude this section by deriving the minimum square error obtained by the application of the optimal kernel, that will be useful for assessing the performance of practical applications of the method. By substituting the expression (4.8) of the optimal kernel in (4.6), the associated minimum square error can be written, after some algebra, as

$$(4.10) \quad \min_K E(I) = \frac{K_{opt}^{(N)}(0) - K_{opt}^{(1)}(0)}{N - 1}$$

where we made explicit the dependence of the optimal kernel on the sample size  $N$ , by writing  $K_{opt} = K_{opt}^{(N)}(x)$ .

Finally, note that  $|\phi(t)|^2 \leq 1$  and  $|\Delta(t)|^2 \leq 1$ , which implies from Eq.(4.9) that also the optimal estimate satisfies  $|\hat{\phi}(t)|^2 \leq 1$ . While this is a necessary condition for the antitransform  $\hat{f}(x)$  to be non-negative, it is not sufficient, and  $\hat{f}(x)$  is not guaranteed to be a non-negative density.

**Appendix 2: Stability of  $\hat{\phi}_{sc}$ .** In this section we derive the expression for the self-consistent estimate  $\hat{\phi}_{sc}$ , Eqs.(2.7,2.8), and we study its stability. We start from Eq.(2.5), the iterative map that we rewrite here

$$(4.11) \quad \hat{\phi}_{n+1} = \frac{N\Delta}{N - 1 + |\hat{\phi}_n|^{-2}}.$$

We search for a fixed point of the iteration, namely  $\hat{\phi}_{sc}$  such that

$$(4.12) \quad \hat{\phi}_{sc} = \frac{N\Delta}{N - 1 + |\hat{\phi}_{sc}|^{-2}}$$

We derive in the following the two solutions (beyond the null solution) of Eq.(4.12) and we show that only one solution is stable with respect to the iteration, Eq.(4.11). We start by taking the absolute value of Eq.(4.12), in order to obtain an equation for the single unknown variable  $|\hat{\phi}_{sc}|$ . Then, we multiply the expression by the denominator and by  $|\hat{\phi}_{sc}|$  (leaving the null solution  $\hat{\phi}_{sc} = 0$ ), obtaining a simple quadratic equation



$$(4.13) \quad (N-1) \left| \hat{\phi}_{sc} \right|^2 + 1 = N |\Delta| \left| \hat{\phi}_{sc} \right|$$

Provided that  $|\Delta|^2 \geq \frac{4(N-1)}{N^2}$ , this equation has the following two solutions, denoted by the superscript  $\pm$

$$(4.14) \quad \left| \hat{\phi}^\pm \right| = \frac{1}{2(N-1)} \left[ N |\Delta| \pm \sqrt{N^2 |\Delta|^2 - 4N + 4} \right]$$

This solution gives only the absolute value of  $\hat{\phi}^\pm$ . By replacing this expression back into the right hand side of Eq.(4.12), we finally obtain the solution for  $\hat{\phi}^\pm$ , given by

$$(4.15) \quad \hat{\phi}^\pm = \frac{2\Delta}{N |\Delta|^2 \mp |\Delta| \sqrt{N^2 |\Delta|^2 - 4N + 4}}$$

Of those two solutions, only one is of interest. First, only  $\hat{\phi}^+$  is normalized, i.e. when  $t = 0$ ,  $\Delta(0) = 1$  implies  $\hat{\phi}^+(0) = 1$ , while  $\hat{\phi}^-(0) = \frac{1}{N-1}$ . The two solutions are of very different magnitudes: for large  $N$  the solution  $\hat{\phi}^-$  quickly vanishes ( $|\hat{\phi}^-| \simeq \frac{1}{N|\Delta|}$ ), while  $\hat{\phi}^+$  stays finite ( $|\hat{\phi}^+| \simeq |\Delta|$ ). In fact, only  $\hat{\phi}^+$  is a stable solution of the iteration, as can be seen by taking the absolute value of Eq.(4.11) and computing the derivative

$$(4.16) \quad \left. \frac{d|\hat{\phi}_{n+1}|}{d|\hat{\phi}_n|} \right|_{|\hat{\phi}_n|=|\hat{\phi}^\pm|} = 1 \mp \sqrt{1 - \frac{4(N-1)}{N^2 |\Delta|^2}}$$

This implies that, provided that the two solutions exist, i.e. provided that  $|\Delta|^2 > \frac{4(N-1)}{N^2}$ , then  $\hat{\phi}^+$  is stable (derivative smaller than one) and  $\hat{\phi}^-$  is unstable (derivative larger than one). When  $|\Delta|^2 = \frac{4(N-1)}{N^2}$ , the two solutions annihilates in a saddle node bifurcation. For  $|\Delta|^2 < \frac{4(N-1)}{N^2}$  only the null solution,  $\hat{\phi}_{sc}=0$ , is available. That is always stable, as can be checked by computing

$$(4.17) \quad \lim_{|\hat{\phi}_n| \rightarrow 0} \frac{d|\hat{\phi}_{n+1}|}{d|\hat{\phi}_n|} = 0$$

If we assume that  $|\hat{\phi}_0| > |\hat{\phi}^-|$ , then the iteration will reach  $\hat{\phi}_{sc} = \hat{\phi}^+$  for  $|\Delta|^2 \geq \frac{4(N-1)}{N^2}$ , and  $\hat{\phi}_{sc} = 0$  for  $|\Delta|^2 < \frac{4(N-1)}{N^2}$ . In the latter case, the null solution is globally stable.

We conclude this section by calculating the mean and variance of the self-consistent estimate  $\hat{f}_{sc}$ , Eq.(2.10). Because  $\hat{\phi}_{sc}$  is continuous and infinitely differentiable at  $t = 0$ , they can be computed by the derivatives of  $\hat{\phi}^+$  and  $|\hat{\phi}^+|^2$  at  $t = 0$ , namely

$$(4.18) \quad E(x) = -i \frac{d\hat{\phi}^+}{dt} \Big|_{t=0} = \frac{d\hat{\phi}^+}{d\Delta} \Big|_{\Delta=1} \left( -i \frac{d\Delta}{dt} \Big|_{t=0} \right)$$

$$(4.19) \quad \text{Var}(x) = -\frac{1}{2} \frac{d^2|\hat{\phi}^+|^2}{dt^2} \Big|_{t=0} = \frac{d|\hat{\phi}^+|^2}{d|\Delta|^2} \Big|_{|\Delta|^2=1} \left( -\frac{1}{2} \frac{d^2|\Delta|^2}{dt^2} \Big|_{t=0} \right)$$

where we used the chain rule and the fact that  $|\Delta|^2$  is an even function, hence  $\frac{d|\Delta|^2}{dt} \Big|_{t=0} = 0$ . It is straightforward to show that the terms in round brackets in Eqs.(4.18,4.19) are, respectively, equal to the sample mean and sample variance. Because  $|\Delta|$  is even, then  $\frac{d\hat{\phi}^+}{d\Delta} \Big|_{\Delta=1} = 1$  and, by differentiating Eq.(4.13), we obtain  $\frac{d|\hat{\phi}^+|^2}{d|\Delta|^2} \Big|_{|\Delta|^2=1} = N/(N-2)$ . Finally, Eqs.(4.18,4.19) can be rewritten as

$$(4.20) \quad E(x) = \frac{1}{N} \sum_{j=1}^N X_j$$

$$(4.21) \quad \text{Var}(x) = \frac{1}{N-2} \sum_{j=1}^N (X_j - E(x))^2$$

**Appendix 3: A sufficient condition for  $\hat{\phi}_{sc} \in \mathbf{L}^2$ .** In this Appendix, we study under which conditions the self consistent estimate  $\hat{\phi}_{sc}$  in Fourier space can be antitransformed back into  $\hat{f}_{sc}$  through Eq.(2.10). This depends on the initial guess  $\hat{\phi}_0$  from which the iteration (2.5) is started. We first study the example discussed in the text, corresponding to  $\hat{\phi}_{sc} = \hat{\phi}^+$  above threshold, and  $\hat{\phi}_{sc} = 0$  below threshold, where the threshold is given by the inequality (2.9). This corresponds to an initial guess  $\hat{\phi}_0$  such that  $|\hat{\phi}_0(t)| > |\hat{\phi}^-(t)|$  for all  $t$ 's whose corresponding amplitude is above threshold. However,

we show in the following that both  $\hat{\phi}_0$  and  $\hat{\phi}_{sc}$  are not in  $L^2$  in that case, and the antitransform of the self-consistent estimate does not exist.

Because the self-consistent estimate in Fourier space is bounded,  $\hat{\phi}_{sc}(t) \leq 1$ , whether it is summable depends on its behavior for large  $|t|$ . In the limit of large  $|t|$ , the Fourier transform of the true distribution vanishes,  $\phi(t) \rightarrow 0$  ( $\phi$  is bounded and summable by assumption), but the probability that the amplitude  $|\Delta(t)|^2$  crosses the threshold remains finite and, in fact, is equal to  $\exp(-4)$ . A straightforward calculation of the moments of  $|\Delta|^2$ , for large  $N$ , gives

$$(4.22) \quad \lim_{|\phi| \rightarrow 0} E(|\Delta|^{2k}) \simeq \frac{k!}{N^{2k}} + O\left(\frac{1}{N^{2k+1}}\right)$$

This implies that, in the above limits, the distribution of amplitudes tends to an exponential distribution, i.e.

$$(4.23) \quad \mathcal{P}(|\Delta|^2 > D) \simeq \exp(-ND)$$

From this expression it is possible to compute the probability of crossing the threshold. For large  $N$ , the threshold expressed by the inequality (2.9) is  $4/N$ , and the probability of that being crossed is  $\mathcal{P}(|\Delta|^2 > 4/N) = \exp(-4)$ . Because this probability does not vanish for large  $|t|$ , the condition  $|\hat{\phi}_0(t)| > |\hat{\phi}^-(t)|$  implies that  $\hat{\phi}_0$  is nonzero, and that a random fluctuation of the amplitude  $|\Delta|^2$  above threshold would determine a nonzero  $\hat{\phi}_{sc}$  for  $|t|$  larger than any arbitrary chosen value. Hence, neither  $\hat{\phi}_0$  nor  $\hat{\phi}_{sc}$  are summable in that case.

However, any summable initial guess  $\hat{\phi}_0 \in L^2$  will converge to a summable self-consistent solution  $\hat{\phi}_{sc} \in L^2$ . Again, because  $\hat{\phi}_{sc} \leq 1$ , whether  $\hat{\phi}_{sc} \in L^2$  depends on its behavior for large  $|t|$ . If  $\hat{\phi}_0 \in L^2$ , it is possible to find a  $t_{max}$  for which  $|\hat{\phi}_0(t)| < |\hat{\phi}^-(t)|$  for all  $|t| > t_{max}$ , which in turn implies  $\hat{\phi}_{sc} = 0$  for all  $|t| > t_{max}$ , and hence  $\hat{\phi}_{sc} \in L^2$ .

**Acknowledgements.** AB would like to thank Alfonso Sutura for introducing him to the issues of nonparametric density estimation. The authors further thank Massimo Cencini, Rishidev Chaudhuri, Andrew Jackson, John Murray, Umberto Picchini and Angelo Vulpiani for their useful comments on a preliminary version of the manuscript.

## REFERENCES

- [1] BERLINET, A. (1993). Hierarchies of higher order kernels. *Probab. Theory Relat. Fields*, **94**, 489-504.

- [2] BIALEK, W., CALLAN, C.G., and STRONG, S.P. (1996). Field theories for learning probability distributions. *Phys. Rev. Lett.*, **77** 4693-4697.
- [3] BINDER, K. (1986). *Monte Carlo methods in statistical physics*. Springer, Verlag NY.
- [4] BOWMAN, A.,W. (1984). An alternative method of cross-validation for the smoothing of density estimates. *Biometrika*, **71** 353-360.
- [5] BREYMAN W., DIAS A., and EMBRECHT P. (2003). Dependence Structures for Multivariate HighFrequency Data in Finance. *Quantitative Finance* **3**(1) 1-14.
- [6] BROWN, E.N., KASS, R.E. and MITRA, P.P. (2004). Multiple neural spike train data analysis: state-of-the-art and future challenges. *Nature Neuroscience* **7**(5) 456-461.
- [7] CLAUSET, A., SHALIZI, C.,R., NEWMAN, M.,E.,J. (2009). Power-law distributions in empirical data. *SIAM Review*, in press.
- [8] DAVIS, K.B. (1977). Mean Integrated Square Error Properties of Density Estimates. *Ann. Stat.* **5** 530-535.
- [9] DEVROYE, L. (1992). A note on the usefulness of superkernels in density estimation. *Ann. Stat.*, **20**, 2037-2056.
- [10] EFROMOVICH, S. (2008). Adaptive estimation of and oracle inequalities for probability densities and characteristic functions. *Ann. Stat.*, **36**, 1127-1155.
- [11] GLAD, I.K., HJORT, N.L., and USHAKOV N.G. (2003) Correction of Density Estimators that are not Densities. *Scand. J. Stat.*, **30**, 415-427.
- [12] GOLDSTEIN, M.L, MORRIS S. A., and YEN G.G. (2004). Problems with fitting to the power-law distribution. *Europ. Phys. J. B* **41** 255-258.
- [13] GOOD, I.J. and GASKINS, R.A. (1971). Nonparametric roughness penalties for probability densities. *Biometrika*, **58** 255.
- [14] HALL, P. and MARRON, J.S. (1987) Choice of kernel order in density estimation. *Ann. Stat.*, **16** 161-173.
- [15] HOLY, T.E. (1997). Analysis of Data from Continuous Probability Distributions. *Phys. Rev. Lett.* **79** 3545-3548.
- [16] HOSSJER O. (1996) Asymptotic bias and variance for a general class of varying bandwidth density estimators. *Probab. Theory Relat. Fields* **105**, 159-192.
- [17] KASS, R. E., VENTURA, V., and BROWN, E. N. (2005). Statistical issues in the analysis of neuronal data. *J Neurophysiol*, **94**(1) 8-25.
- [18] KLEYWEGT G. J. and JONES, T. A. (1996). Phi/Psi-chology: Ramachandran revisited. *Structure* **4**(12) 1395-1400.
- [19] ODLYZKO, A.M. (1987). On the distribution of spacings between zeros of the Zeta function. *Math. Comp.* **48** 273-308.
- [20] OLSON, C.,R., GETTNER, S.N., VENTURA, V., CARTA, R., and KASS, R.E. (2000). Neuronal Activity in Macaque Supplementary Eye Field During Planning of Saccades in Response to Pattern and Spatial Cues. *J. Neurophys.* **84** 1369-1384.
- [21] PARZEN, E. (1962). On estimation of a probability density function and mode. *Ann. Math. Stat.*, **33** 1065-1076
- [22] PERIWAL, V. (1997). Reparametrization Invariant Statistical Inference and Gravity. *Phys. Rev. Lett.*, **78** 4671-4674.
- [23] RIPLEY B. D. and SUTHERLAND I. (1990). Finding spiral structures in images of galaxies. *Phyl. Trans. Roy. Soc.* **332**(1672) pp.477-485.

- [24] RUPPERT, D., and KLINE, B.H. (1994). Bias reduction in kernel density estimation by smoothed empirical transformations. *Ann. Stat.* **22** 185-210.
- [25] SCHMIDT, D.M. (2000). Continuous probability distributions from finite data. *Phys. Rev. E* **61** 1052-1055.
- [26] SCOTT, D. (1979). On optimal and data-based histograms. *Biometrika* **66** 605-610.
- [27] SILVERMAN, B.W. (1986). *Density estimation for statistics and data analysis*. Chapman & Hall.
- [28] WAND, M.P. and JONES, M.C. (1995). *Kernel Smoothing*. Chapman & Hall.
- [29] WATSON, G.S., LEADBETTER, M.R. (1963). On the Estimation of the Probability Density. *Ann. Math. Stat.* **34** 480-491.
- [30] WIENER, N. (1949). *Extrapolation, Interpolation, and smoothing of stationary time series*. New York, Wiley.

DEPARTMENT OF NEUROBIOLOGY,  
YALE UNIVERSITY,  
333 CEDAR STREET, SHM-C400D,  
NEW HAVEN, CONNECTICUT  
E-MAIL: [alberto.bernacchia@yale.edu](mailto:alberto.bernacchia@yale.edu)

THE NIELS BOHR INTERNATIONAL ACADEMY,  
THE NIELS BOHR INSTITUTE, BLEGDAMSVEJ 17,  
DK-2100 COPENHAGEN, DENMARK  
E-MAIL: [pigo@nbi.dk](mailto:pigo@nbi.dk)